Decoding 3D search coil signals in a non-homogeneous magnetic field

Thomassen, J S ; Benedetto, G D ; Hess, B J M

Abstract: We present a method for recording eye-head movements with the magnetic search coil technique in a small external magnetic field. Since magnetic fields are typically non-linear, except in a relative small region in the center small field frames have not been used for head-unrestrained experiments in oculomotor studies. Here we present a method for recording 3D eye movements by accounting for the magnetic non-linearities using the Biot-Savart law. We show that the recording errors can be significantly reduced by monitoring current head position and thereby taking the location of the eye in the external magnetic field into account.

DOI: https://doi.org/10.1016/j.visres.2010.03.017

Decoding 3D search coil signals in a non-homogeneous magnetic field

Jakob S. Thomassen, Giacomo Di Benedetto, Bernhard J.M. Hess

Department of Neurology, University Hospital Zurich

Number of pages (w/ Figures and Tables): 35

Word count (w/o abstract, figure legends and reference list): ~6600

Keywords: eye movement recording; eye-head movements; oculomotor; three-dimensional

Animal classification: non-human primate; rhesus monkey.

Corresponding author:

Dr. Bernhard J.M Hess

Frauenklinikstrasse 26

CH-8091 Zürich

Switzerland

phone: +41-44-255-5500

fax: +41-44-255-4507

E-mail: bhess@neurol.unizh.ch

Abbreviations: 3D, three dimensional; P, Position; E, orientation; STD, standard deviation.

ABSTRACT

We present a method for recording eye–head movements with the magnetic search coil technique in a small external magnetic field. Since magnetic fields are typically non-linear, except in a relative small region in the center small field frames have not been used for head-unrestrained experiments in oculomotor studies.

Here we present a method for recording 3D eye movements by accounting for the magnetic non-linearities using the Biot-Savart law. We show that the recording errors can be significantly reduced by monitoring current head position and thereby taking the location of the eye in the external magnetic field into account.

1. Introduction

In vestibulo-oculomotor studies, rotating or translating devices are often used to stimulate the vestibular sensory organs of the inner ear while monitoring the eye movements. The preferred method for monitoring eye movements is the magnetic search coil technique, which is well established in humans, in non-human primates and other animals (Collewijn, van der Steen, Ferman & Jansen, 1985; Fuchs & Robinson, 1966; Hess, 1990; Judge, Richmond & Chu, 1980; Robinson, 1963). In recent years eye movement recording techniques based on video have gained popularity due to their lesser invasiveness (Houben, Goumans & van der Steen, 2006; Imai, et al., 2005). However, the search coil technique still remains the method of choice for many researchers, due to important advantages such as high spatial and temporal resolution, signal-to-noise ratio, stability, reproducibility and minimal sensitivity to blinking and pupil stability. The search coil technique offers particular and hitherto unmatched advantages in studies of three dimensional (3D) eye movements with or without the head moving.

When using the search coil technique in 3D eye movement studies, a dual search coil consisting of two, roughly, perpendicular coils in a single rigid construction (Collewijn et al., 1985; Hess, 1990) or simply a pair of independent coils (Tweed, Cadera & Vilis, 1990) are used as sensors. In this study we deal solely with the rigid dual search coil, although the method applies in principle also for two independent coils. With the search coil firmly fixed to the eye, the subject is sitting inside a magnetic field that consists of two or three alternating magnetic fields (primary fields) generated by orthogonally arranged external field coils (frame coils). The primary fields induce currents in the two search coils depending on their orientation relative to the primary fields. From these currents the 3D orientation of the search coils (and thus the eye's orientation) can be determined. Since reliable measurements can only be obtained within the region, where the fields

are homogeneous and mutually orthogonal, subjects are typically placed with the head fixed in the center. When measuring eye–head movements, large rectangular frame coils (e.g. 2 × 2 × 2 m) are typically used such that the subject can move its head without leaving the homogeneous part of the field (see e.g. Tweed, Glenn & Vilis, 1995).

To minimize distortions of the primary field, e.g. by the metallic parts in the vicinity, the frame needs to be placed around the head of the subject within a motion device. This imposes considerable restrictions on the size of the frame coils such that eye movements are often not reliably recorded when the subject's head is free to move. Certain geometric frame configurations like the Helmholtz configuration or other configurations with a larger number of frame coils (Collewijn, 1977; Ditterich & Eggert, 2001; Rubens, 1945) provide better linearity than a simple cubic frame, yet at the cost of reducing the subject's field of view. Visuo-vestibular studies typically require the fixation of point targets in far-viewing as visual stimulus and a smaller field of view than the approximate 90° provided by the cube configuration would cause a significant restriction during combined eye–head movement studies.

Here, we present a method for measuring eye movements with the search coil method by taking the non-linear spatial field characteristics into account using the Biot-Savart law. The recording technique was evaluated in two steps: (1) a simulation of eye movements made by an 'artificial eye' which was positioned in various orientations at different locations in the magnetic field and (2) an *in vivo* experiment, where rhesus monkeys were trained to fixate targets with their heads unrestrained. The head movements were measured with an ultrasonic system to locate the spatial eye position in the primary field.

2. Materials and methods

2.1 General experimental setup

For practical purposes, we used two different setups for these experiments. The simulation experiment, which required the manipulation of a three-axis gimbal protractor at different locations, was performed in a large magnetic field frame with side length of 75 cm (Angle-Meter NT, Primelec, Regensdorf, Switzerland). The *in vivo* experiment was done in a similar but much smaller system with side length of approximately 30 cm (Eye Position Meter 3000, Skalar Instruments, Delft, The Netherlands), fitted inside the inner frame of a motorized four-axis gimbaled motion device (Acutrol, Acutronic Schweiz AG, Bubikon, Switzerland). Although the Primelec system is a three-field system generating three primary magnetic fields in contrast to the Skalar system, we used only the output signals of two primary magnetic fields in both sets of experiments (for a three-field approach see Appendix A). One of these fields was directed vertically along the subject's rostro-caudal axis and the other was directed horizontally along the interaural axis of the subject. Physically, each field resulted in fact from superimposing the magnetic fields produced by two parallel-arranged square shaped coils at each side of the frame (Fig. 1). The two coil pairs generated two homogeneous magnetic fields in the center of the frame that were in space quadrature. The Primelec system used frequency encoding to enable separate detection of the fields whereas the Skalar system used phase encoding.

In both sets of experiments, we used the same type of (implantable) dual search coil (Hess, 1990). In brief, the dual search coils consisted of one three-turn wire coil with a diameter of ca. 15 mm (direction coil) and two serially connected oval-shaped miniature wire coils of ca. 1.5 × 2.2 mm diameters and 150 turns each (torsion coil). The torsion coils were rigidly mounted at diametrically opposed positions on the circumference of the direction coil such that the direction of maximal sensitivity was roughly at 90° with respect to the sensitivity direction of the direction coil. The dual

search coil was finally sealed with an electrically insulating Araldite (XD4510, Astorit, Switzerland) and surface coated with a bio-compatible plastic compound (Rilsan PA11, Arkema, France).

All search coil induction data were digitized at 833.33 Hz with a resolution of 12-bit. The data were analyzed offline using MATLAB (The Mathworks Inc., Natrick, MA, USA) and 3D eye orientations were expressed as rotation vectors in space-fixed *x*- (orthogonal to the *y*- and *z*-coordinates), *y*- (interaural axis), and *z*-coordinates (head vertical axis). The eye's orientation while looking straight-ahead was taken as reference position (Haustein, 1989; Hess, Van Opstal, Straumann & Hepp, 1992).

2.2 Search coil signal demodulation using the Biot-Savart law

We used the Biot-Savart law to compute the direction and relative strength of the magnetic field at the position of the search coil (the eye). The rectangular frame coils consisting of straight aluminum bars were approximated by sticks of zero thickness. With this simplification the integration in the Biot-Savart law can be circumvented by using the more computer efficient vector calculations (Haus & Melcher, 1989).

$$H = \frac{i}{4\pi} \frac{c \times a}{|c \times a|^2} \left(\frac{a \bullet c}{|c|} - \frac{a \bullet b}{|b|} \right) \qquad (1)$$

This equation describes the magnetic field vector "*H*" resulting from one of the eight sticks of the frame coils. Each stick is described by a vector, say "*a"* with base at one end of the stick and endpoint at the other end, pointing in the direction of the current flow, denoted by "*i*" (Fig. 1). To compute the magnetic field vector "*H*" at point *P* of the current "*i*" in stick "*a* ", the equation further requires the vector "*b*" with base at point *P* and endpoint at the base of "*a* " and the vector "*c*" with base at *P* and endpoint at the endpoint of vector "*a*". The resulting magnetic field H_{total} can then be

determined by the superposition principle of the eight sticks (or bars) in the frame for each of the coil pairs that generate a primary field. An estimation of the amount of current flow "*i*" is not important because the calculated field does not need to be in absolute values. The field should simply be calculated relative to the center of the frame coils i.e. no correction is made in the center.

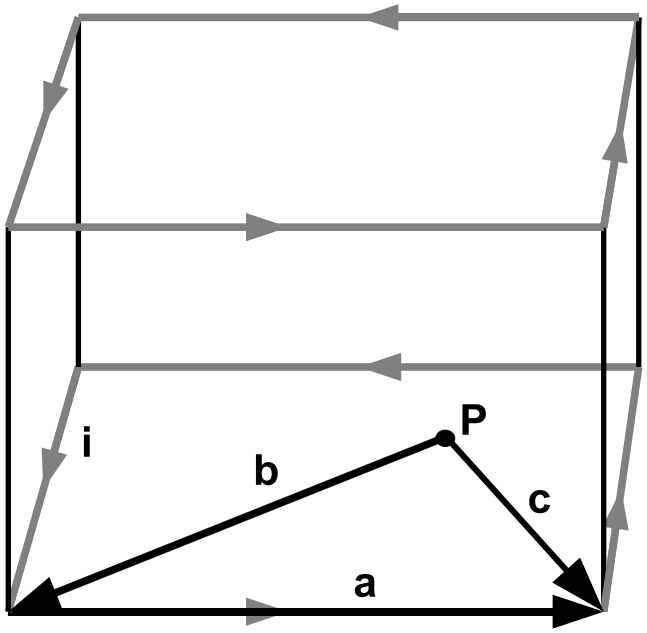

Fig. 1. The magnetic field H_{total} at point P is calculated by superposition of the eight sticks of the two primary coils. It is mainly directed in the vertical direction. The similar calculations are made for the other primary magnetic field which is mainly directed horizontally.

The following describes how to demodulate the search coil signals using only two primary fields (*Y* and *Z*). The procedure for three primary fields (*X*, *Y* and *Z*) is shown in the Appendix A.

We used a right-handed orthogonal coordinate system with positive *x*-direction pointing straight forward (parallel to the naso-occipital axis of the tested subject), positive *y*-direction pointing leftward (parallel to the subject's interaural axis) and the *z*-direction pointing upward (parallel to the subject's rostro-caudal axis). As seen from the subject, positive rotations about the *x*-, *y*- and *z*-axis are clockwise, downward and leftward.

To describe the geometry of the magnetic flow field, we denote the magnetic field vector of

the primary *Y*-field at point *P* by $\vec{v}(P)$. It associates with each point *P* inside the frame coils a vector according to the relation (superscript "*T*" stands for transpose):

$$\vec{v}(P) = [v_1, v_2, v_3]^T \tag{2}$$

Similarly, we denote the magnetic field vectors of the primary *Z*-field at the point P by:

$$\vec{w}(P) = [w_1, w_2, w_3]^T \tag{3}$$

Consider now a search coil, which we will call *direction coil* due to its close alignment with the direction of the line of sight, with the sensitivity vector $\vec{d} = [d_1, d_2, d_3]^T$ (orthogonal to the plane spanned by the search coil) at position *P* in the external field (Fig. 2). The sensitivity vector carries information about the magnitude of the induced currents measured in the center of the external field (i.e. calibration at point *P* = 0) and the present direction of the coil. The induced output signals, d_v and d_w, at any position $P = [x_P, y_P, z_P]$ in the external field can be obtained by taking the dot products of the sensitivity vector and the respective magnetic field $\vec{v}(P)$ and $\vec{w}(P)$:

$$d_v(P,E) = \vec{d}(E) \bullet \vec{v}(P) = d_1 \cdot v_1 + d_2 \cdot v_2 + d_3 \cdot v_3 \tag{4}$$

$$d_w(P,E) = \vec{d}(E) \bullet \vec{w}(P) = d_1 \cdot w_1 + d_2 \cdot w_2 + d_3 \cdot w_3 \tag{5}$$

Note that field vectors $\vec{v}(P)$ and $\vec{w}(P)$ are normalized by the magnitudes calculated at the center of the frame coils (*P* = 0). The dummy variable "*E*" refers to the fact that these signals depend on eye orientation when the coil is fixed to the eye.

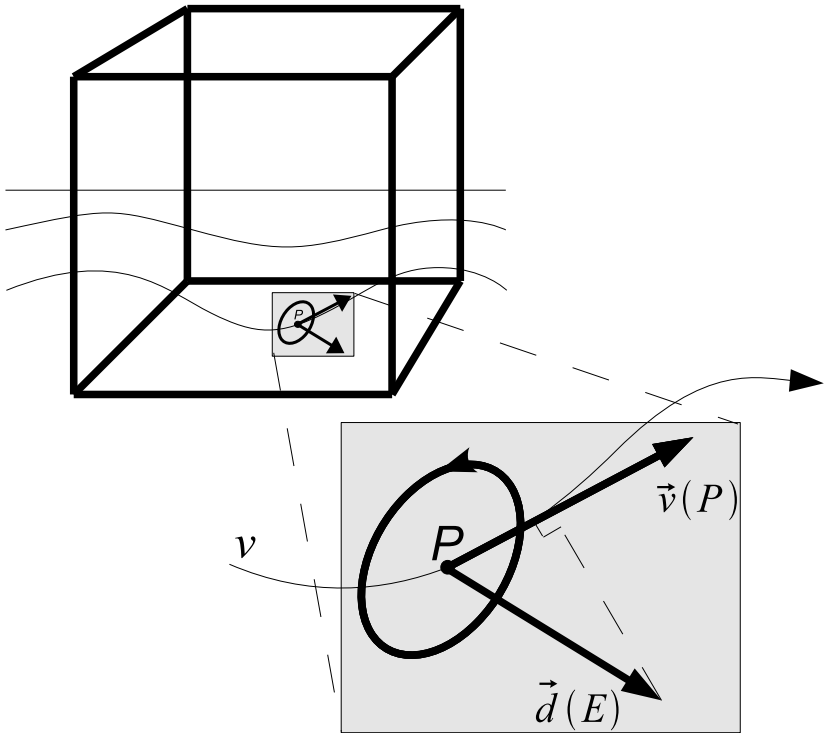

Fig. 2. A magnetic search coil inserted at point P in the alternating magnetic field "v" will pick up an alternating current. The induced current will be proportional to the dot product of the sensitivity vector "$\vec{d}(E)$" (perpendicular to the plane of the coil windings) and the magnetic field vector of the alternating field "$\vec{v}(P)$" at the location P (see inset showing the direction coil represented by vector $\vec{d}(E)$).

To measure the 3D orientation of the eye we need information from two search coils, which must be fixed to the eye ball in non-parallel planes. Thus, the second search coil, called *torsion coil*, with the sensitivity vector $\vec{t} = [t_1, t_2, t_3]^T$ should not be parallel to the first coil but rather perpendicular to it for optimal 3D decoding. The output signals t_v and t_w of the torsion coil can likewise be written as functions of the direction and position of the coil in the external field:

$$t_v(P,E) = \vec{t}(E) \bullet \vec{v}(P) = t_1 \cdot v_1 + t_2 \cdot v_2 + t_3 \cdot v_3 \tag{6}$$

$$t_w(P,E) = \vec{t}(E) \bullet \vec{w}(P) = t_1 \cdot w_1 + t_2 \cdot w_2 + t_3 \cdot w_3 \tag{7}$$

As in the previous two equations the dummy variable "*E*" stands for eye position. Eqs. (4) and (5) can be solved for d_2 and d_3, and Eqs. (6) and (7) can be solved for t_2 and t_3:

$$d_2 = d_1 \cdot a_2 + b_{2d} \tag{8}$$

$$d_3 = d_1 \cdot a_3 + b_{3d} \tag{9}$$

$$t_2 = t_1 \cdot a_2 + b_{2t} \tag{10}$$

$$t_3 = t_1 \cdot a_3 + b_{3t} \tag{11}$$

where, $a_2 = \frac{v_1 \cdot w_3 - w_1 \cdot v_3}{w_2 \cdot v_3 - v_2 \cdot w_3}$, $a_3 = \frac{v_2 \cdot w_1 - w_2 \cdot v_1}{w_2 \cdot v_3 - v_2 \cdot w_3}$, $b_{2d} = \frac{d_w \cdot v_3 - d_v \cdot w_3}{w_2 \cdot v_3 - v_2 \cdot w_3}$,

$b_{3d} = \frac{d_v \cdot w_2 - d_w \cdot v_2}{w_2 \cdot v_3 - v_2 \cdot w_3}$, $b_{2t} = \frac{t_w \cdot v_3 - t_v \cdot w_3}{w_2 \cdot v_3 - v_2 \cdot w_3}$, and $b_{3t} = \frac{t_v \cdot w_2 - t_w \cdot v_2}{w_2 \cdot v_3 - v_2 \cdot w_3}$.

Assuming a rigid geometric configuration of the direction search coil, the sensitivity, represented by the vector length, can be obtained *a priori* from a calibration of the search coil at the center of the field (for details see Section 2.5):

$$\left|\vec{d}\right| = \sqrt{d_1^{\,2} + d_2^{\,2} + d_3^{\,2}} \quad \text{(measured at } P = 0\text{)} \tag{12}$$

Then d_1 can now be found by substituting Eqs. (8) and (9) in Eq. (12):

$$a \cdot d_1^{\,2} + b_d \cdot d_1 + c_d = 0 \tag{13}$$

where $a = 1 + a_2^{\,2} + a_3^{\,2}$, $b_d = 2 \cdot a_2 \cdot b_{2d} + 2 \cdot a_3 \cdot b_{3d}$ and $c_d = b_{2d}^{\,2} + b_{3d}^{\,2} - \left|\vec{d}\right|^2$

Solving Eq. (13) yields two solutions for d_1 with opposite signs. The actual sign depends on the winding direction of coil, which can be determined from the calibration. It is important to note that a two field system with primary fields in *y*- and *z*-directions, as indicated in Eqs. (4) and (5), only allows measurements of less than ±90° from the *x*-direction for the direction coil and loses accuracy when approaching this limit. The limit can also be described by a plane spanned by the *y*- and *z*-directions. Direction coil directions beyond the limit are indistinguishable from those within the limit and will therefore by itself be assumed to be within the limit. In practice, it is the torsion coil of the dual search sensor that will reveal if the limit is exceeded.

Because of this limitation of a two field system it is not possible to reliably predict t_1 from the vector length since this coil is likely to operate close to the plane spanned by the *y*- and *z*-directions. However, by assuming that the relative orientation of the torsion and direction coils remains constant, we can use the information about the configuration of the coil vectors from the calibration to calculate the angle ρ between the two coils:

$$\cos(\rho) = \left(d_1 \cdot t_1 + d_2 \cdot t_2 + d_3 \cdot t_3\right) \Big/ \left(|\vec{d}| \cdot |\vec{t}|\right) \text{ (measured at } P = 0) \tag{14}$$

And by substituting Eqs. (10) and (11) in Eq. (14), we obtain for:

$$t_1 = \frac{|\vec{d}||\vec{t}|\cos(\rho) - d_2 \cdot b_{2t} - d_3 \cdot b_{3t}}{d_1 + d_2 \cdot a_2 + d_3 \cdot a_3} \tag{15}$$

Finally t_2 and t_3 are obtained from Eqs. (10) and (11).

Because of the geometry underlying Faraday's law of induction, the structure of the rotation matrix is closely related to the search coil vectors. Even though we will ultimately use rotation vectors for describing the eye orientation the most straightforward way to evaluate the search coil signals is in the format of 3 × 3 rotation matrices using Euler angles before transforming them into other representations (see Appendix A for a short review of the definition and properties of rotation vectors).

The rotation matrix describes the 3D orientation relative to the field frame by three orthonormal vectors in right-handed orientation. Thus the first column simply is the normalized direction coil vector:

$$\hat{d} = \left[\hat{d}_1, \hat{d}_2, \hat{d}_3\right]^T = \vec{d} \Big/ \left|\vec{d}\right| \tag{16}$$

The second column is the unit vector that aligns with the direction of the projection of the torsion coil vector onto the plane orthogonal to the direction coil vector. With $\hat{t} = \vec{t}/|\vec{t}|$ we have:

$$\hat{t}^{\perp} = \left(\hat{t} - \hat{d}\cos(\rho)\right) \Big/ \left|\hat{t} - \hat{d}\cos(\rho)\right| \tag{17}$$

Finally, the last column-vector, which must be orthogonal to the first two column-vectors, is the cross product of the first and second column. Thus, the resulting rotation matrix at point *P* reads:

$$R(P) = \begin{bmatrix} \hat{d}_1 & \hat{t}_1^{\perp} & \left(\hat{d} \times \hat{t}^{\perp}\right)_1 \\ \hat{d}_2 & \hat{t}_2^{\perp} & \left(\hat{d} \times \hat{t}^{\perp}\right)_2 \\ \hat{d}_3 & \hat{t}_3^{\perp} & \left(\hat{d} \times \hat{t}^{\perp}\right)_3 \end{bmatrix} \tag{18}$$

Note that this rotation matrix describes the orientation of the dual search coil relative to the magnetic field frame, which is not necessarily aligned with gaze direction. The orientation of the eye relative to the dual search coil can be determined from a calibration (see Section 2.5).

2.3 Biot-Savart based- versus experimentally measured magnetic field characteristics

To compare the calculated field based on the Biot-Savart law with the actual magnetic field characteristics we used a custom-made robot that systematically moved three mutually orthogonal single search coils (diameters of 20 mm) inside the magnetic field frame. We recorded the 3D linear positions of the search coils together with the induced currents at every second centimeter in the *x*-, *y*- and *z*-directions in one octant of the Primelec system and mirrored the data to the other octants in order to map out the magnetic field. The measured magnetic field vectors were then normalized to unity at the center of the primary fields and interpolated (cubic spline) to obtain an estimate of the magnetic field at the relevant positions inside the field frame. Based on these measurements, the magnetic field was used to demodulate search coil signals in a similar way as described for the calculated field in the previous section (using the Biot-Savart law). A comparison between the two methods was made with the data recorded in the simulation experiment described in the following section.

2.4 Validation procedures based on simulated 3D eye positions

This procedure was used to measure the quality of the theoretically calculated and robot measured magnetic fields in terms of precision and accuracy of 3D eye position demodulation. For this, we mounted a test dual search coil on a three-axis gimbal protractor, which could be rotated through any angle in horizontal, vertical and torsional directions (for a description of the nesting of the gimbal axes see Hess et al., 1992). The protractor was tracked with an optical position measurement system for precise positioning inside the magnetic field (OPTOTRAK 3020, Northern Digital, Canada).

We recorded the induced output for nine different orientations of the dual search coil: reference orientation (0° for all axes) and all combinations of ±30° horizontal, ±30° vertical and ±20° torsional directions (see Table 2 in Hess et al., (1992)). The orientation was determined by reading off the values on each axis of the gimbal protractor. This procedure was repeated at each of 25 positions in the *x-y* plane (Fig. 3A), as well as at 3 additional positions towards the upper right front corner of the magnetic field frame (Fig. 3B, positions FRU1, FRU2 and FRU3), giving a total of 252 samples (9 x 28) for each of the three dimensions (horizontal, vertical, and torsional).

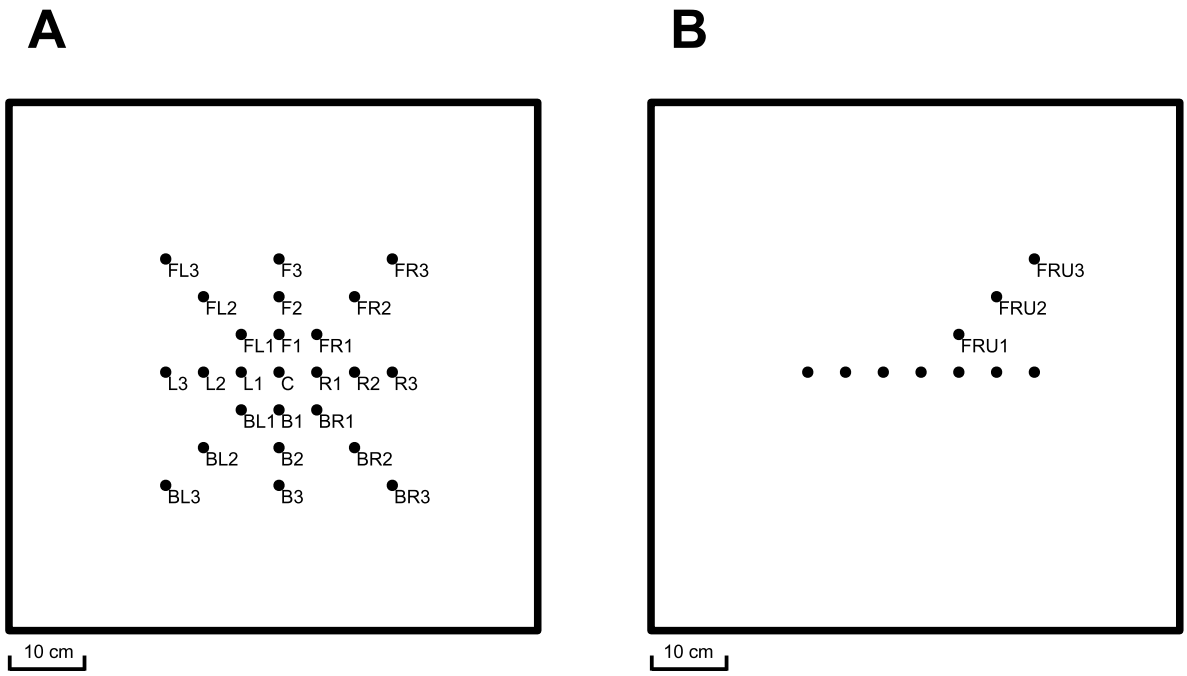

Fig. 3. (A) Top-view of the 25 positions in the horizontal plane where the gimbal was placed. The 30 × 30 cm measured plane cuts though the center of the field frame with side lengths of 75 × 75 × 75 cm. (B) Behind-view of the three additional positions recorded towards the upper right front corner. The seven unlabeled dots indicate the edge-on view of the plane of 25 positions shown in (A).

In the *x*- and *y*- direction, the field was measured every 5 cm whereas along the diagonal (in the *x*-*y* plane) recordings were made at intervals of 7.1 cm (i.e. displaced 5 cm in the *x*- and 5 cm in the *y*-direction). Positions along the *z*-direction (above the *x*-*y* plane) were likewise spaced out at 5 cm intervals, yielding diagonal intervals between recording points in the *x*-, *y*- and *z*-direction of $\sqrt{5^2+5^2+5^2}cm \approx 8.66cm$. For each position with each orientation of the dual search coil, the difference between the actual orientation on the gimbal protractor and the predicted orientation from the induced currents was compared, with and without using the Biot-Savart based demodulation or by using demodulation based on the experimentally measured magnetic field.

2.5 Calibration of dual search coil parameters with two primary fields

In contrast to systems with three primary fields, 3D search coil recordings in systems with only two primary fields require a precalibration to characterize the sensitivities and mutual orientations of the two coils constituting the dual search coil. This precalibration, also called *in vitro* calibration needs to be done prior to applying the coil on the eye and requires a rigidly assembled dual search coil. We thus determined the sensitivity of each of the two search coils, and the angle between them by measuring the induced currents after rotating the dual search coil with the help of a gimbal protractor in the center of the field frame to known orientations. The orientation of a dual search coil (on the eye/gimbal) was determined by a second calibration, called *in vivo* calibration, during which the subject with the head at rest fixated vertical targets placed in the sagittal plane though the eye at known vertical angles. Because only two of the three components of the orientation of the search coil are captured by a two field system, the third component had to be computed from the predetermined sensitivities of the direction and torsion coil in the *in vitro* calibration. For a complete and detailed explanation of these procedures see Hess et al., (1992) and for calibration of non-rigid search coils see e.g. Bartl, Siebold, Glasauer, Helmchen & Buttner, (1996).

Although it is not always possible to situate the subject so that the eye with the search coil is exactly in the center of the primary fields during the calibrating procedure, this usually poses no problems as long as the subsequent experiments are performed in the same position. In head-unrestrained experiments, however, it is desirable to obtain the calibration parameters from the center of the magnetic fields because offset voltages, which are not related to the coil orientation in the magnetic fields, can only then be distinguished from the non-linear distortions. To overcome this problem we introduced a recursive method to estimate the offset voltages even when the calibration was performed in the non-linear part of the magnetic field. In an initial step, the Biot-

Savart correction was applied to the raw output signals; the offsets were calculated and subtracted from the raw output. In the subsequent steps, this procedure was repeated as follows: the Biot-Savart correction was applied now to the (first order) offset-corrected output signals, new offset voltages were computed and the summed (first and second order) offset voltages were subtracted again from the raw output signals. This recursive loop was run until the Biot-Savart corrected output signals yielded near zero (high-order) offset voltages (Fig. 4). As a consequence, the recursively computed coil parameters and the accumulated offsets reached values after the last iteration as if the calibration was done in the center of the magnetic field. A reasonable accuracy is usually obtained after about 4–5 iterations.

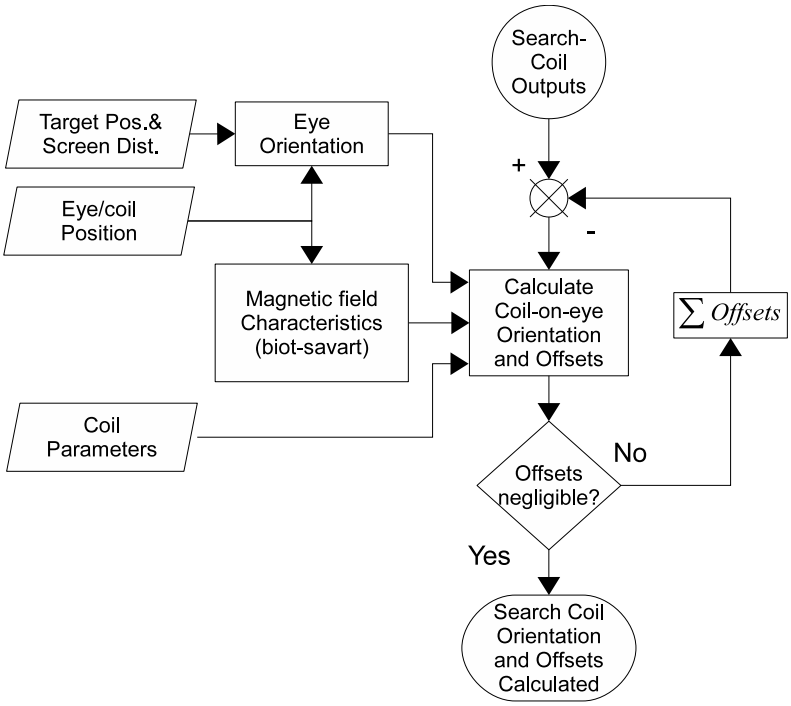

Fig. 4. Functional block diagram of the procedure for obtaining calibration parameters. The calibration parameters are calculated by correcting the entire search coil output measured in the non-linear part of the magnetic field and are then corrected recursively to minimize the offsets.

2.6 Validation procedures based on eye–head movement recordings in non-human primates

Four female rhesus monkeys (Macaca mulatta, body weights 5–6 kg), prepared with skull bolts for

head restraint, were used in these validation procedures as an integral part of a larger project with wider scope. Dual search coils were implanted on one eye under general anesthesia as described in Hess, (1990). All procedures and animal care protocols accorded with the NIH Guide for the Care and Use of Laboratory Animals and were approved by the Veterinary Office of the Canton of Zürich. The animals were trained to fixate nine targets, presented sequentially at locations forming a 3x3 matrix with equally spaced rows and columns ranging from –20° to 20°, using a custom-made software package based on Spike2 that controlled LED point targets, the reward delivery and the data acquisition (1401*plus* and Spike2, Cambridge Electronic Design Ltd., Cambridge, England).

The head position and orientation was recorded using a compact ultrasonic tracking device (CMS 20, Zebris Medical GmbH, Isny, Germany). To ensure undisturbed data recording the head position data was routed through a dedicated PC to ensure stable data rate at 200Hz before being forwarded via a DAC to the main acquisition hardware.

Three ultrasonic emitters were rigidly mounted to the subject's head to measure the translation and rotation of the head. From this, the spatial position of the eye (and thus of the dual search coil) was calculated relative to the field frame. The calculated magnetic field characteristics at the current location of the dual search coil was then used to determine the exact orientation of the coil relative to the external field frame, from which eye-in-space orientation relative to gaze straight-ahead was determined. To reward the animal for accurate target fixation, the search coil signals were demodulated online according to the current spatial position of the eye in the magnetic field. Horizontal and vertical gaze directions, recorded at the time of fixation, were evaluated off line with- and without the Biot-Savart based demodulation. The gaze was corrected for the effect of parallax due to a translation of eye relative to the space-fixed targets. Three dimensional eye movements were measured but the accuracy and precision were only evaluated for the horizontal and vertical directions (relative to the target positions). The torsional eye components in this *in vivo*

experiment lack the presence of a natural reference since the head was free to move, i.e. Listing's law was not obeyed (Collewijn et al., 1985; Glenn & Vilis, 1992; Hess, 2008). Fig. 5 shows a diagram of the steps necessary for calculating the current gaze direction from the recorded search coil and head position sensor signals.

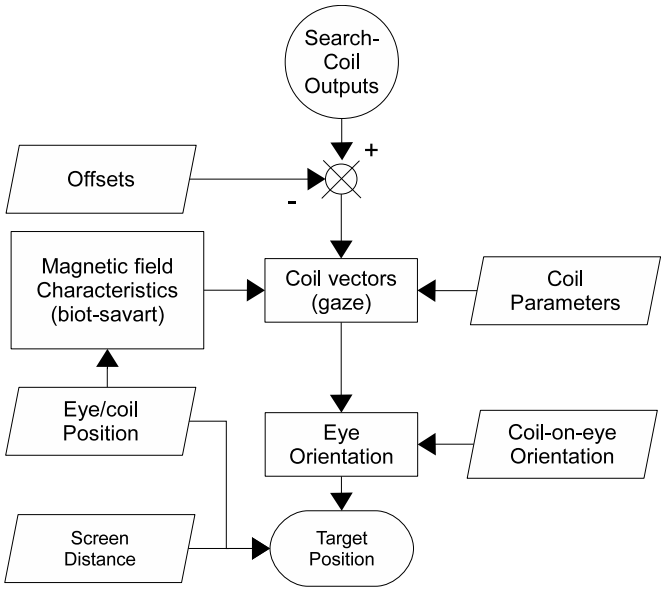

Fig. 5. Functional block diagram showing the practical algorithm used for calculating the angular direction of the target that the eye was fixating. The rhomboids denote input parameters and the rectangular boxes denote the algorithm.

3. Results

3.1 Biot-Savart based demodulation of simulated 3D eye position measurements

The data for the 28 positions in the primary field was collected in 10 groups according to their distance to the center: In the center (group A), at the positions F1, R1, B1 and L1 which were all 5 cm from the center (group B, see Fig 3A), and likewise in the other positions with matching distances to the center (collected in groups C thru J, see Fig 3A and B and inset in Fig. 6).

As expected, the error increased relatively rapidly relative to the distance to the center (thick curve in Fig. 6). The data corrected with the Biot-Savart-based demodulation (thin solid curve), however, showed a significant improvement in the accuracy (P<0.05, Wilcoxon signed-rank) for all

groups, except the center group, which had a P-value of 1 as expected since no correction was performed at this position. The error scores at individual positions, without grouping, were also significantly improved, except at positions F1, FL1 and B1.

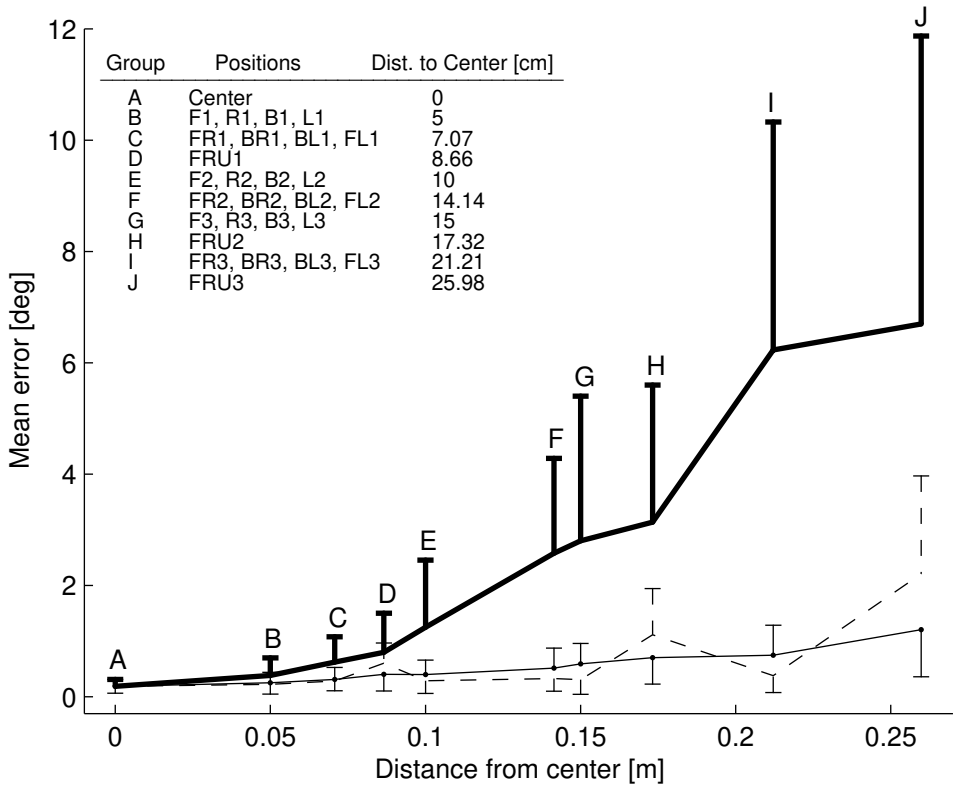

Fig. 6. Average demodulation error expressed as difference between actual and demodulated direction of a test coil at positions ordered by distance to center. The thick curve shows the uncorrected demodulation (assuming linear field characteristics), the thin solid curve shows Biot-Savart corrected demodulation and the dashed curve shows the errors when using the experimentally measured field characteristics. Error bars are one standard deviation. Inset: Table of groups with matching distance to the center.

The correction performance was considerable for all three dimensions of rotation as demonstrated in Fig. 7, which shows a box plot of the grouped data separated in each of the three dimensions. The horizontal lines in each box denote the median, the upper- and the lower quartiles. The whiskers from the boxes show the minimum and maximum error measured. The upper row shows the uncorrected errors for each of the three directions, horizontal, vertical and torsional. The respective

plots for the Biot-Savart based corrected errors are shown in the three lower plots. It is remarkable that in this 75 cm field frame already positions further than only 15 cm from the center gave very unpredictable measurements with occasionally more than 10° and more than 3° error on average when the magnetic field non-linearities were not taken into account.

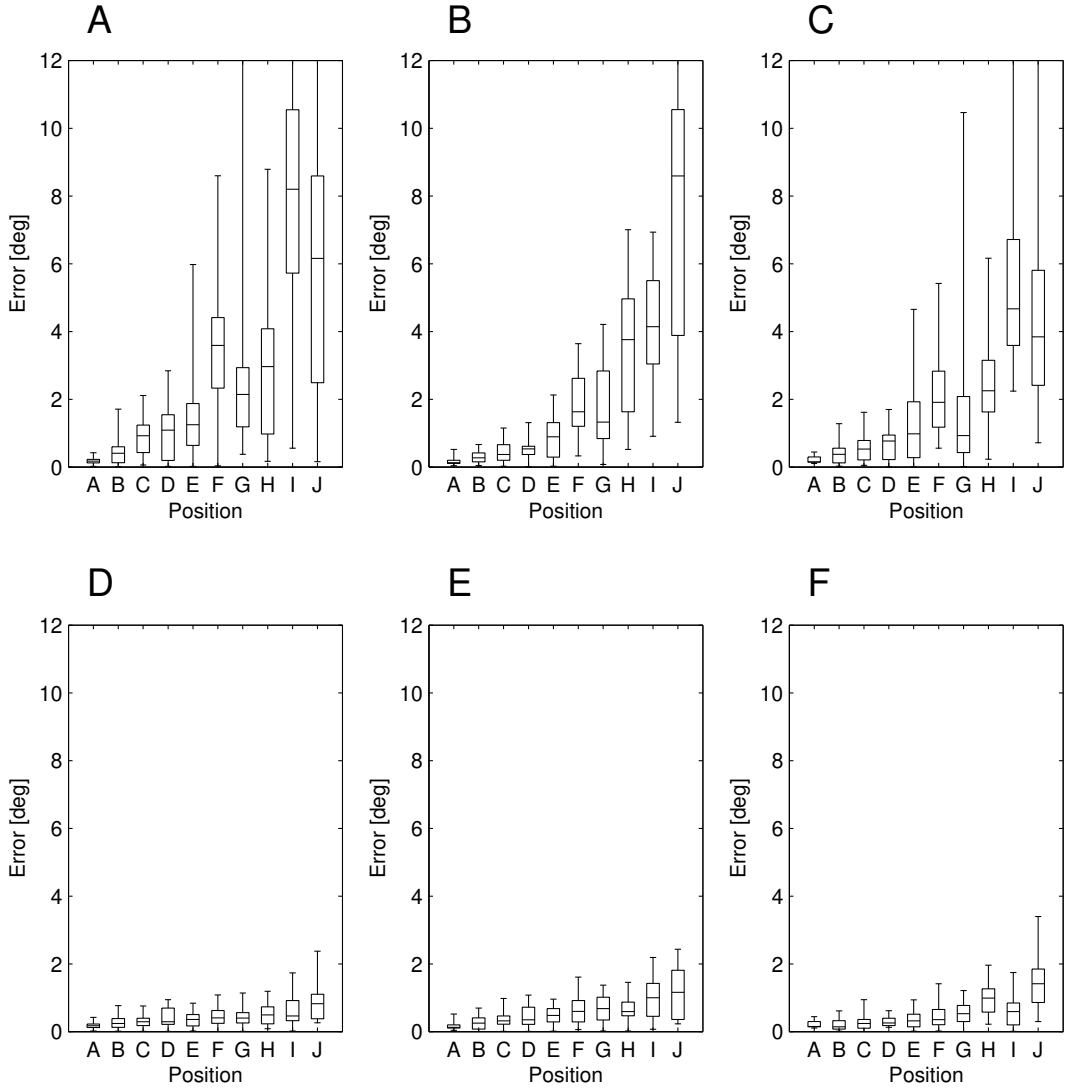

Fig. 7. Box plot showing the error of the demodulation. Subplot A, B and C show horizontal, vertical and torsional errors, respectively, when the data was not corrected. D, E and F are the same but showing errors after Biot-Savart based correction. Position A shows the error measured in the center of the field. Positions B thru J shows the errors at the grouped positions in order of distance to the center (see table inset in Fig. 6).

3.2 Biot-Savart based- versus experimentally measured magnetic field characteristics

To compare the two approaches we used the data from the simulated 3D eye positions and demodulated it using the experimentally measured magnetic field characteristics in a similar way as was done when using the Biot-Savart based calculations. This showed no significant overall difference in performance between the two procedures (dashed versus solid curve in Fig 6), although the Biot-Savart procedure seems to have a more stable increase in error versus distance to center and to perform better for the three groups D, H and J, which are the positions towards upper right front corner but slightly worse for the other groups (the positions in the *x*-*y* plane).

3.3 Biot-Savart based demodulation of eye–head movement recordings in non-human primates

The *in vivo* experiments showed significant improvements in the measured accuracy of fixations performed during head movements when applying the described method. The mean errors for corrected and uncorrected fixations measured in four animals for the nine fixation targets were in the range of 0.64–0.93º and 1.56–4.89º respectively. The uncorrected error depended highly on the relative contribution of the head to the gaze movement. Although the targets were well within the oculomotor range (±20º) so that it was not necessary to move the head, all four animals typically used also the head to variable degrees to fixate the targets. As indicated by the data in Table 1, subjects P and M moved the head less than subjects X and L for the same task.

Subject	No. of fixations	Uncorrected Mean error ± STD	Corrected Mean error ± STD
P	136	1.91 ± 0.67°	0.93 ± 0.48°
M	155	1.56 ± 0.85°	0.64 ± 0.40°
X	24	4.89 ± 1.77°	0.93 ± 0.51°
L	102	4.13 ± 1.94°	0.59 ± 0.35°

Table 1: Mean errors and standard deviations for fixations in the four subjects.

The error score for uncompensated fixations, defined as the distance in degrees between the target and the calculated fixation point, originated from a lack of both accuracy and precision. The accuracy, which can be described as a general shift of the fixation points relative to the target of interest, had two sources (Fig. 8A): A common shift of eye position of the individual trials for each target due to the correlation of the mean spatial eye position with target position. E.g. when the target was to the left, the subject generally tended to turn the head to the left, which translated the eye to the left side of the field frame, causing parallax and distortion due to the non-linearity of the magnetic field. The second source, causing a general shift, came from the fact that the overall average of spatial eye positions during the experiments was different from the position where the calibration (with the head restrained) was obtained. To minimize this bias, we attempted to restrain the head in a position as natural (and comfortable for the animal) as possible, in order to obtain the calibration as close as possible to the mean position that the animal was going to assume during the head-unrestrained experiments. A third source of error in the uncompensated fixations was the precision, or the scatter of the fixation directions aimed at a particular target, which reflects the scatter in spatial eye positions for that particular target. This can also be described as biological noise, since it is a consequence of the variation in the ratio of eye and head movement. That is, for a given target fixation the contribution of head movement can be small and the eye movement large or vice versa. As seen in Fig. 8B, the algorithm improves both accuracy and precision.

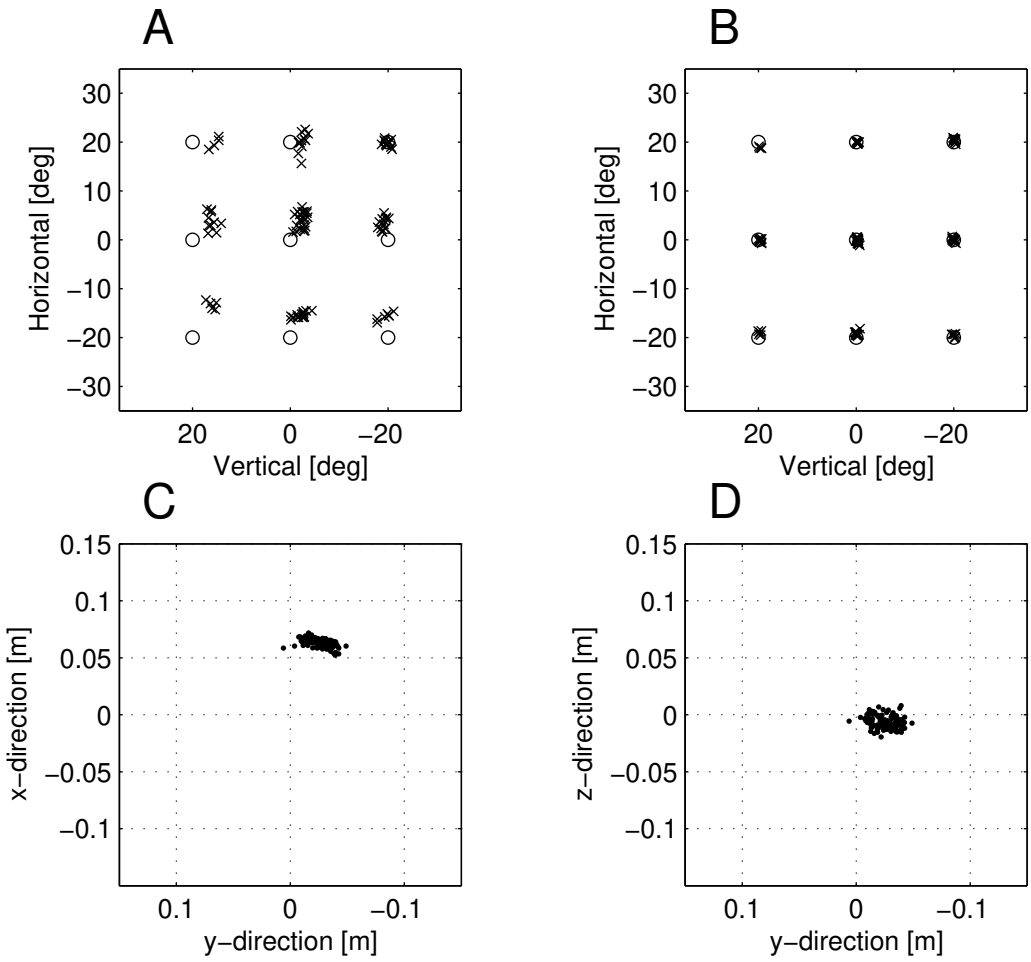

Fig. 8. One-hundred and two fixations, marked by crosses, made by subject 'L' towards nine targets marked by circles. (A) Uncorrected fixations. (B) Biot-Savart based corrected fixations. (C and D) Top view and behind view, respectively, of eye positions in the magnetic field at the time of the fixations.

4. Discussion and Conclusions

We have quantified the errors in 3D eye movement recordings obtained in the head-unrestrained rhesus monkey during a fixation task, using the magnetic search coil technique in a cubic primary field frame of only 30cm side length. We developed a method that efficiently minimizes the errors by accounting for the characteristic non-linearities of the magnetic field by using the Biot-Savart law. We show that by this method 3D eye movements can be recorded in the head-unrestrained rhesus monkey during a fixation task with nearly the same precision and accuracy as when 3D eye movements were recorded in the center of the magnetic field, which typically requires restraining head movements.

In the *in vivo* experiments the location of the eye in the external field was on average 4–7 cm from the field center of the 30 cm cubic frame. In comparison with the 75 cm field frame, which was used in the *simulations*, these distances translate into 10–17.5 cm. Comparing the average errors at comparable distances from the field center, there is a good correspondence between the errors measured in the *in vivo* and the *simulation* experiments, suggesting that the errors found in the *simulation* can serve as a predictor of the errors in *in vivo* recordings (see Fig. 6). The robot-controlled measurements mapping out the magnetic field characteristics offer no practical advantage over calculating the field characteristics with the more effortless ‘stick method’. The here presented Biot-Savart demodulation technique allows one to perform eye–head movement studies at sufficiently high precision in all degrees of rotational and translational freedom within relatively compact primary magnetic field frames.

Alternatively to our approach several other studies have shown that artificial neural networks, trained with back propagation on a subset of sampled fixation data, can be used to calibrate eye movements or eye-head movements in 2D, at least in the homogeneous range of the

magnetic field (Bremen, Van der Willigen & Van Opstal, 2007; for EOG measurements: Coughlin, Cutmore & Hine, 2004; Goossens & Van Opstal, 1997). In fact, a similar procedure could be used for calibrating the 2D eye movements in the non-homogeneous range. A difficulty in applying this approach for calibration of 3D eye position would be to specify appropriate assumptions about the torsion that the eye assumes during 2D gaze shifts in the head-free condition. Without such assumptions training of the artificial neural network on a subset of all accessible targets would not yield physiologically meaningful torsion. The reason for this is that although it is not possible to voluntarily control ocular torsion during target fixation, the actual amount of torsion is in general not only a function of gaze direction but depends also on other parameters like head orientation relative to gravity or other vestibular signals. Since our primary interest was to develop a model-free calibration method in order to be able to study gaze control in stationary as well as non-stationary environments, an implementation of artificial neural network techniques was beyond the focus of this study.

Real-time application of the here presented Biot-Savart demodulation technique depends on measuring online head position within the field frame. For this we used a small-sized sensor system, using travel time measurements of ultrasonic pulses, which fitted in the limited space available above the subjects head. The main disadvantage of this solution is the relatively narrow temporal bandwidth due the comparably slow sonic travel speed. An elegant way to overcome this restriction would be to equip the conventional two-field system used here for measuring 3D eye movements with a gradient magnetic field along the third dimension (*x*-direction). As shown by Schilstra & van Hateren, (1998a, 1998b), such a configuration would in fact allow one to measure head orientation and position with a 3D miniature sensor mounted on the subject's head. Thus, this technique for measuring head position (and orientation) in combination with the here presented Biot-Savart demodulation technique in a conventional two-field system, using an easy implantable dual search

coil, can be used for reliably measuring 3D eye position during head-free gaze shifts irrespective of the off-center magnetic field non-linearity.

5. Acknowledgments

The authors would like to thank U. Scheifele, C. Bettoni and B. Disler for technical assistance with the experiments and animal care. This work was supported by the Betty and David Koetser Foundation for Brain Research and GdB (now at Dept. of Mechanics, Politecnico di Torino) and JT were fellows of the European Commissions Marie-Curie Action (FP6) under Contract No. MEST-CT-2004-007825.

Appendix A

A.1 Search coil signal demodulation using three primary fields

For the primary field generated in the *x*-direction, we denote the magnetic field vector calculated at point *P* by the function (superscript "*T*" stands for transpose):

$$\vec{u}(P) = [u_1, u_2, u_3]^T \tag{19}$$

Similarly, for the primary field generated in the *y*-direction:

$$\vec{v}(P) = [v_1, v_2, v_3]^T \tag{20}$$

And the field generated *z*-direction:

$$\vec{w}(P) = [w_1, w_2, w_3]^T \tag{21}$$

For simplicity we summarize these three functions in a matrix, called *Biot-Savart matrix*, as follows:

$$[M_{BS}]_P = [\vec{u}, \vec{v}, \vec{w}]^T{}_P$$

Consider now a search coil, called *direction coil*, with a sensitivity vector $\vec{d} = [d_1, d_2, d_3]^T$ (orthogonal to the plane spanned by the coil) at position *P* in the external field (Fig. 2) which describes the coils direction relative to the field frame. The induced current output $\vec{D}(P,E) = [d_u, d_v, d_w]_{P,E}$ of this coil is a function of its position $P = [x_P, y_P, z_P]$ in the magnetic field and can be described by the dot product of the sensitivity vector and the magnetic field vector for each field:

$$\begin{aligned} d_u(P,E) &= \vec{d}(E) \bullet \vec{u}(P) \\ d_v(P,E) &= \vec{d}(E) \bullet \vec{v}(P) \\ d_w(P,E) &= \vec{d}(E) \bullet \vec{w}(P) \end{aligned} \qquad (22)$$

The dummy variable "*E*" in these equations indicates that the direction of the sensitivity vector $\vec{d}$ in the field in fact depends on eye position because the direction coil is supposed to be firmly fixed to the eye. Together with a second search coil, it is possible to describe the orientation (*E*) of the eye relative to the field frame. Thus, to measure 3D orientation of the eye we need information from a second search coil, which must be fixed to the eye ball such that the two coil vectors span a plane. The optimal orientation of the second search coil, called *torsion coil*, with sensitivity vector $\vec{t} = [t_1, t_2, t_3]^T$ is in a plane perpendicular to the first one. The output signal $\vec{T}(P,E) = [t_u, t_v, t_w]_{P,E}$ of the torsion coil can likewise be written as functions of the direction and position of the coil in the external field:

$$\begin{aligned} t_u(P,E) &= \vec{t}(E) \bullet \vec{u}(P) \\ t_v(P,E) &= \vec{t}(E) \bullet \vec{v}(P) \\ t_w(P,E) &= \vec{t}(E) \bullet \vec{w}(P) \end{aligned} \qquad (23)$$

The set of equations in (22) and (23) is a system of linear equations for the vectors $\vec{d}(E)$ and $\vec{t}(E)$. Summarizing the functions $\vec{u}(P)$, $\vec{v}(P)$ and $\vec{w}(P)$ in the Biot-Savart matrix $[M_{BS}]_P$ we

can write the solutions to (22) and (23) as:

$$\vec{d}(E) = \left[M_{BS}\right]_P^{-1} \cdot \vec{D}(P,E)$$
$$\vec{t}(E) = \left[M_{BS}\right]_P^{-1} \cdot \vec{T}(P,E) \qquad (24)$$

From these two coil sensitivity vectors we can calculate the rotation matrix as described in Section 2.2.

A.2 Demodulation of simulated 3D eye position measurements using three primary fields

Like for the two field evaluation the mean errors and standard deviations of three-field evaluation was increasing rapidly with distance from the center although the general error score was lower (compare thick lines in Figs. 6 and 9). Small decreases in the mean error scores were also found for the Biot-Savart based demodulation and the one based on the experimentally measured magnetic field characteristics when compared with the two field evaluation.

The decrease of error scores for the Biot-Savart based corrected data when compared with the uncorrected data was significant for all groups ($P < 0.01$), except in the center position as expected ($P = 1$). The error scores at individual positions, without grouping, were also significantly improved, except for F1 and FL1.

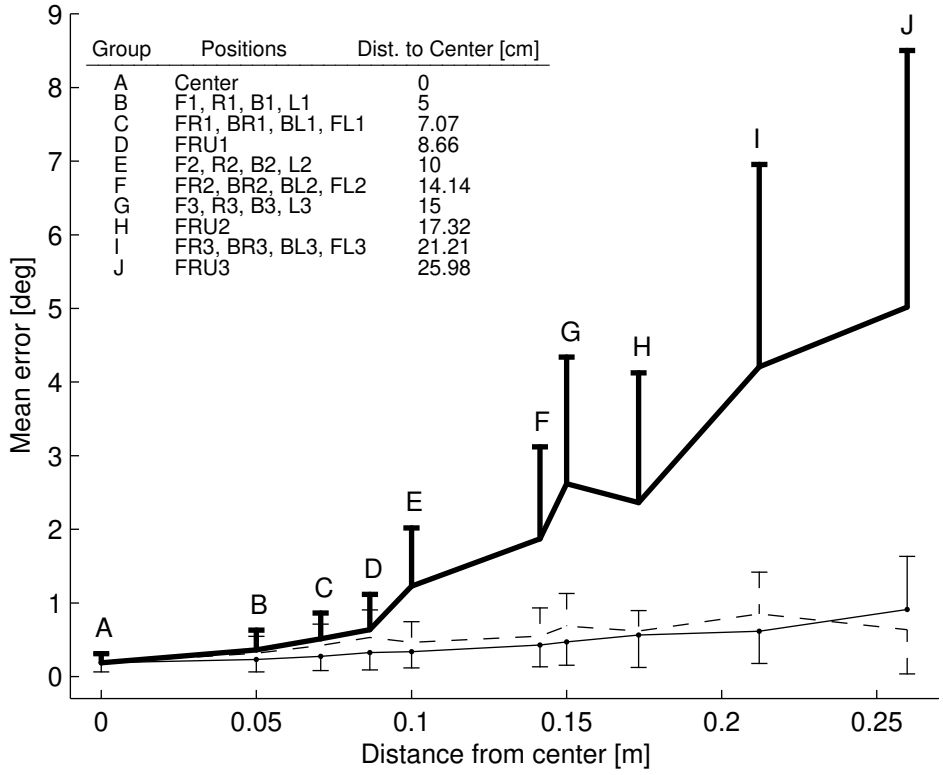

Fig. 9. Average demodulation error using three primary fields. The thick curve shows the uncorrected demodulation, the thin solid curve shows Biot-Savart corrected demodulation and the dashed curve shows the errors when using the experimentally measured field characteristics.

A.3 Simulation of 3D eye position data during head-free gaze movements

This section describes the simulation of 3D eye position data used to verify the described Biot-Savart decoding algorithm and search coil demodulation procedure. The eye was simulated to be directed towards nine targets at locations forming a 3 × 3 matrix with equally spaced rows and columns (–20°, 0° and 20°). The head was simulated to be located in the center of the frame coils such that its yaw plane was parallel to the *x*-*y* plane of the field frame and the naso-occipital axis intersected the central target (0°). The eye (dual search coil) was simulated to be located at $x = 4.5$ cm (forward positive) and $y = –1.5$ cm (left positive), corresponding roughly to the proportions of the rhesus monkeys used for the *in vivo* experiments. The gaze movements were simulated as

random rotations of the head and eye such that the head contributed on average 80% of the gaze movement (normal distribution with $\mu_{head} = 0.8 \times$ target angle, standard deviation $\sigma_{head} = 10°$). We evaluated a total of 135 simulated fixations (15 fixations for each of the nine different target positions), for which the head contribution was used to determine the location of the eye and, accounting for parallax, calculated the gaze-on-target directions relative to a spherical screen with radius 88 cm, surrounding in its center the frame coils. From the orientation and location of the eye we calculated the induced currents in the search coils as outlined in Fig. 10.

The orientation of the dual search coil relative to the eye was simulated with data from a calibration of a test coil where the relationship was defined by a rotation matrix. From this rotation matrix we derived the direction coil sensitivity vector from the first column which corresponds to the direction coil defined as a unit vector, multiplied by the sensitivity:

$$\vec{d} = \hat{d} \cdot \left| \vec{d}_{pre} \right| \tag{25}$$

The subscript "pre" indicates that in *in vivo* experiments the sensitivity is determined before the search coil is implanted as described in Section 2.5. From the second column of the calibration rotation matrix, which is the normalized orthogonal component of the torsion coil sensitivity vector, we derived the vector as follows:

$$\vec{t} = \hat{t} \cdot \left| \vec{t}_{pre} \right| \text{ with } \hat{t} = \left(\hat{t}^{\perp} + \hat{d} / \tan(\rho) \right) \Big/ \left| \hat{t}^{\perp} + \hat{d} / \tan(\rho) \right| \tag{26}$$

where ρ was the angle between the direction and torsion coil vector. The two vectors were then rotated as required to hit the target:

$$\begin{aligned} \vec{d}_{gaze} &= R_{gaze} \, \vec{d} \\ \vec{t}_{gaze} &= R_{gaze} \, \vec{t} \end{aligned} \tag{27}$$

R_{gaze} is the rotation matrix describing the eye's orientation. The coil vectors were multiplied with the Biot-Savart matrix at the given field position:

$$\vec{d}_{BS} = M_{BS}\ \vec{d}_{gaze}$$
$$\vec{t}_{BS} = M_{BS}\ \vec{t}_{gaze} \tag{28}$$

from which the induced output current was derived after adding the offsets voltages:

$$\vec{d}_{out} = \vec{d}_{BS} + \vec{d}_{offset}$$
$$\vec{t}_{out} = \vec{t}_{BS} + \vec{t}_{offset} \tag{29}$$

The simulated output was then demodulated as described in Section 2.2 and the gaze direction was compared with the target position for accuracy.

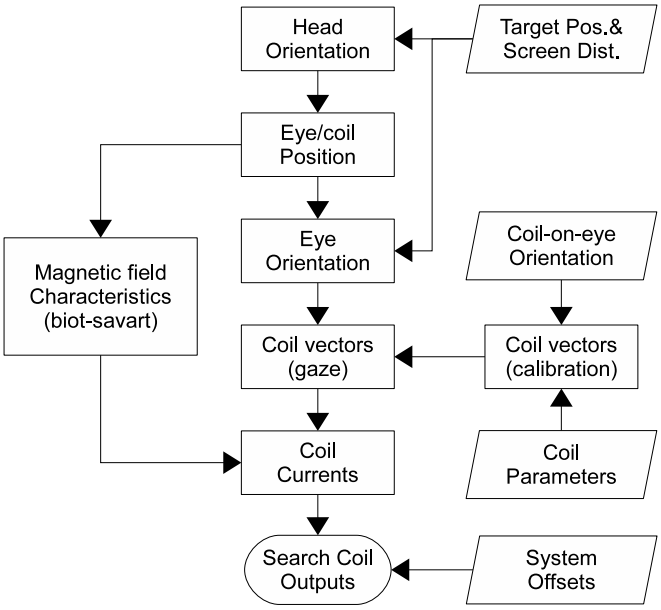

Fig. 10. Functional block diagram showing the algorithm used to simulate the current induced in the search coil. The Rhomboids denotes input parameters and the rectangular boxes denote the algorithm.

A.4 Biot–Savart based demodulation of simulated eye–head movement recordings.

We applied the same algorithm as used in the *in vivo* experiments to the simulated induced currents for calculating the gaze direction. Since the magnetic field calculations used in the simulation for the induced currents were the same as the ones for the reconstruction, the errors for corrected fixations were, as expected, very low (on average close to machine precision). The uncorrected fixations showed a mean error of 2.49 ± 1.03° comparable to the ones found in the *in*

vivo experiments. The gaze directions for corrected and uncorrected fixations are shown along with the spatial location of the eye at the time of fixation in Fig. 11.

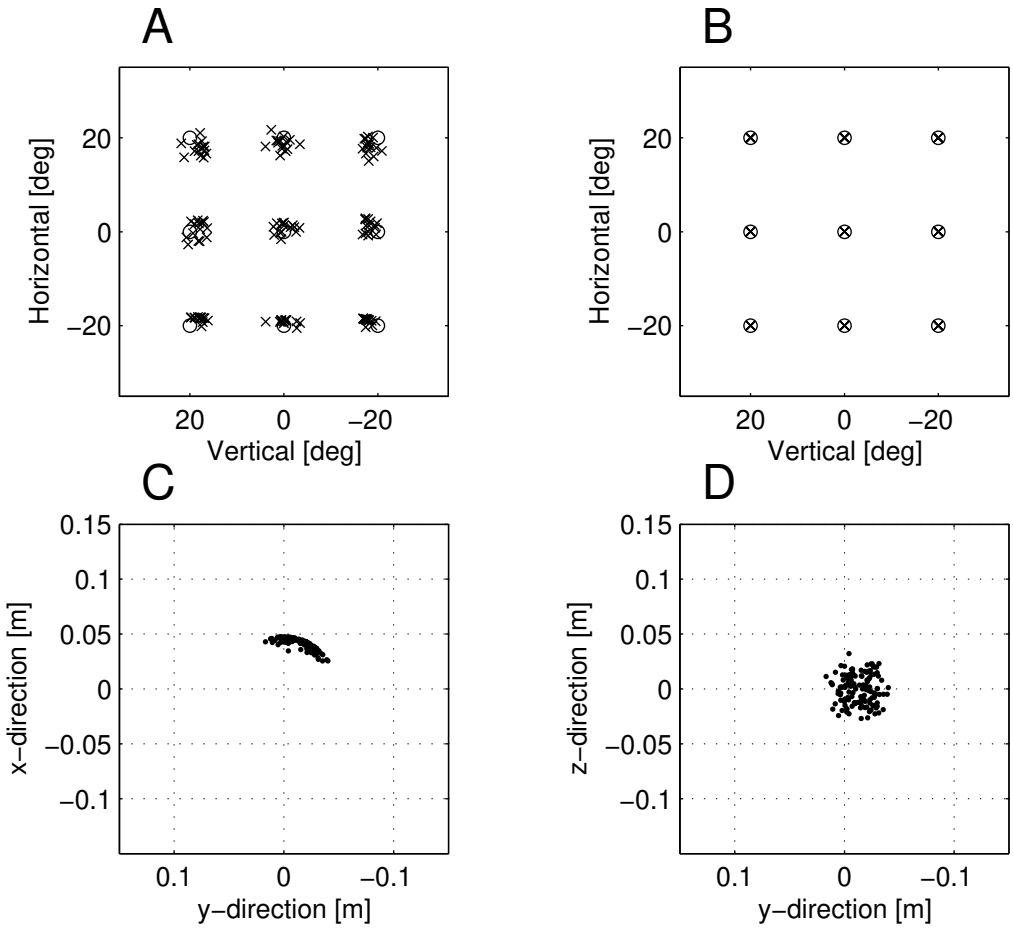

Fig. 11. Eye–head movement computer simulations. Nine targets marked by circles and 135 fixations marked by crosses (simulated with 0.8 head-eye ratio and 10° STD head rotation). (A) Uncorrected fixations. (B) Biot-Savart based corrected fixations. (C) and (D) Top view and behind view, respectively, of eye positions in the magnetic field at the time of the fixations.

A.5 Properties of the rotation vector

A rotation R in 3D space can be described by a 3×3 matrix, whose components are restricted by the requirement of orthogonally. Another way to express 3D rotations is by exploiting the fact that any 3D rotation can be characterized by an axis or unity vector (which is in fact the real

eigenvector of the associated rotation matrix) and a rotation angle (corresponding to the associated eigenvalue). Thus, a rotation vector is a vector ($\vec{r}$) that represents the axis of rotation and, by its length, the angle of rotation (Haustein, 1989). The polarity of the vector describes the direction of the rotation by the right hand rule (thumb of right hand pointing in direction of the vector and the fingers curl in the direction of the rotation). The rules of combining rotations require that the length of the rotation vector is set as the tangent of half the angle of rotation: $|\vec{r}| = \tan(\theta/2)$. The conversion between rotation matrix and rotation vector uses the fact that $\vec{r}$ is an eigenvector of *R*. With $\alpha = 1 + R_{11} + R_{22} + R_{33}$ one obtains $r_1 = (R_{32} - R_{23})/\alpha$, $r_2 = (R_{13} - R_{31})/\alpha$ and $r_3 = (R_{21} - R_{12})/\alpha$, where R_{ik} is defined as the matrix element in row "*i*" and column "*k*": $R_{ik} = [R]_{ik}$. The angle of rotation θ is defined by $\theta = \arccos((R_{11} + R_{22} + R_{33} - 1)/2)$.

Inverse rotations are obtained by taking the transpose of the rotation matrix $R^{-1}=R^{T}$ with $[R^{T}]_{ik} = [R]_{ki}$. As seen from the above relations, this translates into simply taking the negative rotation vector ($r^{-1} = -r$). It can be useful to combine consecutive rotations (Haustein, 1989; Hepp, 1990). For example, when calculating the eye orientation relative head orientation ($\vec{r}_{EH}$) when eye and head orientations are both recorded relative to the field frame (eye-in-space: $\vec{r}_{ES}$ and head-in-space: $\vec{r}_{HS}$, respectively).

$$\vec{r}_{EH} = \vec{r}_{HS}^{\,-1} \circ \vec{r}_{ES} = \frac{\vec{r}_{ES} - \vec{r}_{HS} + \vec{r}_{ES} \times \vec{r}_{HS}}{1 + \vec{r}_{ES} \bullet \vec{r}_{HS}} \qquad (30)$$

REFERENCES

Bartl, K., Siebold, C., Glasauer, S., Helmchen, C., & Buttner, U. (1996). A simplified calibration method for three-dimensional eye movement recordings using search-coils. *Vision Res, 36* (7), 997-1006.

Bremen, P., Van der Willigen, R.F., & Van Opstal, A.J. (2007). Using double-magnetic induction to measure head-unrestrained gaze shifts. I. Theory and validation. *J Neurosci Methods, 160* (1), 75-84.

Collewijn, H. (1977). Eye- and head movements in freely moving rabbits. *J.Physiol (Lond), 266* (2), 471-498.

Collewijn, H., van der Steen, J., Ferman, L., & Jansen, T.C. (1985). Human ocular counterroll: assessment of static and dynamic properties from electromagnetic scleral coil recordings. *Exp.Brain Res., 59* (1), 185-196.

Coughlin, M.J., Cutmore, T.R., & Hine, T.J. (2004). Automated eye tracking system calibration using artificial neural networks. *Comput Methods Programs Biomed, 76* (3), 207-220.

Ditterich, J., & Eggert, T. (2001). Improving the homogeneity of the magnetic field in the magnetic search coil technique. *IEEE Trans Biomed Eng, 48* (10), 1178-1185.

Fuchs, A.F., & Robinson, D.A. (1966). A method for measuring horizontal and vertical eye movement chronically in the monkey. *J Appl Physiol, 21* (3), 1068-1070.

Glenn, B., & Vilis, T. (1992). Violations of Listing's law after large eye and head gaze shifts. *J Neurophysiol, 68* (1), 309-318.

Goossens, H.H., & Van Opstal, A.J. (1997). Human eye-head coordination in two dimensions under different sensorimotor conditions. *Exp Brain Res, 114* (3), 542-560.

Haus, H.A., & Melcher, J.R. (1989). Electromagnetic Fields and Energy. (Englewood Cliffs, NJ: Prentice Hall.

Haustein, W. (1989). Considerations on Listing's Law and the primary position by means of a matrix description of eye position control. *Biol.Cybern., 60* (6), 411-420.

Hepp, K. (1990). On listing's law. *Commun.Math.Phys, 132*, 285-292.

Hess, B.J. (1990). Dual-search coil for measuring 3-dimensional eye movements in experimental animals. *Vision Res, 30* (4), 597-602.

Hess, B.J. (2008). Control of ocular torsion in the rotational vestibulo-ocular reflexes. *Prog Brain Res, 171*, 199-206.

Hess, B.J., Van Opstal, A.J., Straumann, D., & Hepp, K. (1992). Calibration of three-dimensional eye position using search coil signals in the rhesus monkey. *Vision Res, 32* (9), 1647-1654.

Houben, M.M., Goumans, J., & van der Steen, J. (2006). Recording three-dimensional eye movements: scleral search coils versus video oculography. *Invest Ophthalmol Vis Sci, 47* (1), 179-187.

Imai, T., Sekine, K., Hattori, K., Takeda, N., Koizuka, I., Nakamae, K., et al. (2005). Comparing the accuracy of video-oculography and the scleral search coil system in human eye movement analysis. *Auris Nasus Larynx, 32* (1), 3-9.

Judge, S.J., Richmond, B.J., & Chu, F.C. (1980). Implantation of magnetic search coils for measurement of eye position: an improved method. *Vision Res, 20* (6), 535-538.

Robinson, D.A. (1963). A Method of Measuring Eye Movement Using a Scleral Search Coil in a Magnetic Field. *IEEE Trans Biomed Eng, 10*, 137-145.

Rubens, S.M. (1945). Cube-Surface Coil for Producing a Uniform Magnetic Field. *Rev Sci Instr., 16* (9), 243-245.

Schilstra, C., & van Hateren, J.H. (1998a). Stabilizing gaze in flying blowflies. *Nature, 395* (6703), 654.

Schilstra, C., & van Hateren, J.H. (1998b). Using miniature sensor coils for simultaneous measurement of orientation and position of small, fast-moving animals. *J Neurosci Methods, 83* (2), 125-131.

Tweed, D., Cadera, W., & Vilis, T. (1990). Computing three-dimensional eye position quaternions and eye velocity from search coil signals. *Vision Res, 30* (1), 97-110.

Tweed, D., Glenn, B., & Vilis, T. (1995). Eye-head coordination during large gaze shifts. *J Neurophysiol, 73* (2), 766-779.